Supplementary Information

Angular and temperature dependence of current induced spin-orbit effective fields in Ta/CoFeB/MgO nanowires

Xuepeng Qiu[1], Praveen Deorani[1], Kulothungasagaran Narayanapillai[1], Ki-Seung Lee[2,3], Kyung-Jin Lee[2,3,4], Hyun-Woo Lee[5] & Hyunsoo Yang[1]

[1]*Department of Electrical and Computer Engineering, National University of Singapore, 117576, Singapore*

[2]*Department of Materials Science and Engineering, Korea University, Seoul 136-701, Korea*

[3]*Spin Convergence Research Center, Korea Institute of Science and Technology, Seoul 136-791, Korea*

[4]*KU-KIST Graduate School of Converging Science and Technology, Korea University, Seoul 136-713, Korea*

[5]*PCTP and Department of Physics, Pohang University of Science and Technology, Kyungbuk 790-784, Korea*

S1. Second harmonic component V_{2f} of the Hall voltage V_{H}

With an ac current with a frequency f applied through the nanowire, the magnetization oscillation can be decomposed and characterized by $\Delta\theta$ and $\Delta\phi$. Considering both anomalous and planar Hall effects (AHE and PHE, respectively), the Hall voltage V_{H} can be written as

$$V_H = V_{AHE} + V_{PHE} = I_{ac} \sin \omega t R_{AHE} \sin(\theta + \Delta\theta \sin \omega t)$$
$$+ I_{ac} \sin \omega t R_{PHE} \cos^2 \left(\theta + \Delta\theta \sin \omega t\right) \sin\left(2\left(\phi + \Delta\phi \sin \omega t\right)\right)$$

where $\omega = 2\pi f$.

By using Taylor expansion, $f\left(x+\delta\right) = f\left(x\right) + f'\left(x\right)\cdot\delta + f''\left(x\right)\cdot\frac{\delta^2}{2} + \ldots$, one can get

$\sin(\theta + \Delta\theta \sin \omega t) = \sin\theta + \cos\theta\Delta\theta \sin \omega t + \ldots$.

Therefore, V_{AHE} can be written as

$$V_{AHE} = I_{ac} \sin \omega t R_{AHE} \sin(\theta + \Delta\theta \sin \omega t) = I_{ac} \sin \omega t R_{AHE} (\sin\theta + \cos\theta\Delta\theta \sin \omega t)$$
$$= I_{ac} R_{AHE} \sin\theta \sin \omega t + I_{ac} R_{AHE} \cos\theta\Delta\theta \sin^2 \omega t$$
$$= I_{ac} R_{AHE} \sin\theta \sin \omega t + \frac{I_{ac} R_{AHE} \cos\theta\Delta\theta}{2} - \frac{I_0 R_{AHE} \cos\theta\Delta\theta}{2} \cos 2\omega t$$

The second harmonic term of V_{AHE} is

$$V_{2f,AHE} = -\frac{I_{ac} R_{AHE} \cos\theta\Delta\theta}{2} \tag{S1.1}$$

When magnetic field is applied in *x*-*z* plane ($\phi = 0°$), by using Taylor expansion, one can get

$$\cos^2 \left(\theta + \Delta\theta \sin \omega t\right) = \left(\cos\theta - \sin\theta\Delta\theta \sin \omega t - \cos\theta \frac{\Delta\theta^2 \sin^2 \omega t}{2} + \ldots \right)^2$$
$$\sin\left(2\left(\phi + \Delta\phi \sin \omega t\right)\right) = \sin\left(2\Delta\varphi \sin \omega t\right) = 2\sin\left(\Delta\varphi \sin \omega t\right)\cos\left(\Delta\varphi \sin \omega t\right) = 2\Delta\varphi \sin \omega t$$

Therefore, V_{PHE} can be written as

$$V_{PHE} = I_{ac} \sin \omega t R_{PHE} \cos^2 \left(\theta + \Delta\theta \sin \omega t\right) \sin(2\Delta\phi \sin \omega t)$$
$$= I_{ac} \sin \omega t R_{PHE} \left(\cos\theta - \sin\theta\Delta\theta \sin \omega t - \cos\theta \frac{\Delta\theta^2 \sin^2 \omega t}{2} + \ldots \right)^2 2\Delta\varphi \sin \omega t$$
$$= 2 I_{ac} R_{PHE} \cos^2 \theta 2\Delta\varphi \sin^2 \omega t$$
$$= I_{ac} R_{PHE} \cos^2 \theta\Delta\varphi - I_{ac} R_{PHE} \cos^2 \theta\Delta\varphi \cos 2\omega t$$

In this geometry with $\phi = 0°$, the second harmonic term of V_{PHE} is

$$V_{2f,PHE} = -I_{ac}R_{PHE} \cdot \cos^2\theta \cdot \Delta\varphi \tag{S1.2}$$

When magnetic field is applied in *y*-*z* plane ($\phi = 90°$), by using Taylor expansion, one can get

$$\cos^2\left(\theta + \Delta\theta \sin\omega t\right) = \left(\cos\theta - \sin\theta\Delta\theta \sin\omega t - \cos\theta\frac{\Delta\theta^2 \sin^2\omega t}{2} + \ldots\right)^2$$

$$\sin\left(2\left(\phi + \Delta\phi \sin\omega t\right)\right) = 2\sin\left(90° + \Delta\varphi \sin\omega t\right)\cos\left(90° + \Delta\varphi \sin\omega t\right)$$

$$= -2\sin\left(\Delta\varphi \sin\omega t\right)\cos\left(\Delta\varphi \sin\omega t\right) = -2\Delta\varphi \sin\omega t$$

Therefore, V_{PHE} can be written as

$$V_{PHE} = I_{ac} \sin\omega t R_{PHE} \cos^2\left(\theta + \Delta\theta \sin\omega t\right)\sin(2(90° + \Delta\phi \sin\omega t))$$

$$= -I_{ac} \sin\omega t R_{PHE}\left(\cos\theta - \sin\theta\Delta\theta \sin\omega t - \cos\theta\frac{\Delta\theta^2 \sin^2\omega t}{2} + \ldots\right)^2 2\Delta\varphi \sin\omega t$$

$$= -2I_{ac}R_{PHE} \cos^2\theta 2\Delta\varphi \sin^2\omega t$$

$$= -I_{ac}R_{PHE} \cos^2\theta\Delta\varphi + I_{ac}R_{PHE} \cos^2\theta\Delta\varphi \cos 2\omega t$$

In this geometry with $\phi = 90°$, the second harmonic term of V_{PHE} is

$$V_{2f,PHE} = I_{ac}R_{PHE} \cdot \cos^2\theta \cdot \Delta\varphi \tag{S1.3}$$

Combining equations of S1.1 ~ S1.3, with inclusion of contributions from anomalous and planar Hall effects, the second harmonic term V_{2f} of V_H can be expressed as

$$V_{2f,//} = -\frac{I_{ac}R_{AHE}\cos\theta\Delta\theta}{2} - I_{ac}R_{PHE}\cos^2\theta\Delta\phi \quad (\text{H in } x\text{-}z \text{ plane, } \phi = 0°)$$

and (S1.4)

$$V_{2f,\perp} = -\frac{I_{ac}R_{AHE}\cos\theta\Delta\theta}{2} + I_{ac}R_{PHE}\cos^2\theta\Delta\phi \quad (\text{H in } y\text{-}z \text{ plane, } \phi = 90°)$$

S2. Relation between the magnetization direction and current induced spin-orbit effective fields

With the ac current induced effective fields, equations of magnetization direction and current induced effective fields are derived by solving the force balance equation along the $\hat{x}\times\hat{m}$ and $\hat{y}\times\hat{m}$ directions.

First, with the coordinate system as defined in Fig. 1(b), the magnetization direction can be expressed as $\hat{m} = (\cos\theta\cos\phi, \cos\theta\sin\phi, \sin\theta)$, $\hat{x}\times\hat{m}$, and $\hat{y}\times\hat{m}$, where

$$\hat{x}\times\hat{m} = \begin{pmatrix} i & j & k \\ 1 & 0 & 0 \\ \cos\theta\cos\phi & \cos\theta\sin\phi & \sin\theta \end{pmatrix} = (0, -\sin\theta, \cos\theta\sin\phi)$$

$$\hat{y}\times\hat{m} = \begin{pmatrix} i & j & k \\ 0 & 1 & 0 \\ \cos\theta\cos\phi & \cos\theta\sin\phi & \sin\theta \end{pmatrix} = (\sin\theta, 0, -\cos\theta\cos\phi).$$

Then, the anisotropy field and current induced effective fields can be expressed as

$$\begin{aligned} \hat{H}_{an} &= H_{an}(0,0,\sin\theta) \\ \hat{H}_L &= H_L \frac{\hat{y}\times\hat{m}}{|\hat{y}\times\hat{m}|} = \frac{H_L}{\sqrt{\sin^2\theta + \cos^2\theta\cos^2\phi}}(\sin\theta, 0, -\cos\theta\cos\phi) \\ \hat{H}_T &= H_T(0,1,0) \end{aligned}$$

(1) When magnetic field is applied in the *x*-*z* plane

In this geometry, $\hat{H} = H(\cos\theta_H, 0, \sin\theta_H)$. The force balance equations along $\hat{x}\times\hat{m}$ and $\hat{y}\times\hat{m}$ are

$$\begin{aligned} &\left(\hat{H} + \hat{H}_L + \hat{H}_T + \hat{H}_{an}\right)\cdot\left(\hat{x}\times\hat{m}\right) \\ &= H\sin\theta_H\cos\theta\sin\phi - \frac{H_L}{\sqrt{\sin^2\theta + \cos^2\theta\cos^2\phi}}\left(-\cos^2\theta\sin\phi\cos\phi\right) \\ &-H_T\sin\theta + H_{an}\sin\theta\cos\theta\sin\phi \\ &= 0 \end{aligned} \qquad \text{(S2.1)}$$

$$\begin{aligned}&\left(\hat{H}+\hat{H}_L+\hat{H}_T+\hat{H}_{an}\right)\cdot\left(\hat{y}\times\hat{m}\right)\\&=H\cos\theta_H\sin\theta-H\cos\theta\cos\phi\sin\theta_H-H_L\sqrt{\sin^2\theta+\cos^2\theta\cos^2\phi}\\&-H_{an}\cos\theta\sin\theta\cos\phi\\&=0\end{aligned}\tag{S2.2}$$

(2) When magnetic field is applied in the *y*-*z* plane

In this geometry, $\hat{H}=H(0,\cos\theta_H,\sin\theta_H)$. The force balance equations along $\hat{x}\times\hat{m}$ and $\hat{y}\times\hat{m}$ are

$$\begin{aligned}&\left(\hat{H}+\hat{H}_L+\hat{H}_T+\hat{H}_{an}\right)\cdot\left(\hat{x}\times\hat{m}\right)\\&=H\cos\theta_H\sin\theta-H\cos\theta\sin\phi\sin\theta_H+\frac{H_L}{\sqrt{\sin^2\theta+\cos^2\theta\cos^2\phi}}\left(-\cos^2\theta\sin\phi\cos\phi\right)\\&+H_T\sin\theta-H_{an}\sin\theta\cos\theta\sin\phi\\&=0\end{aligned}\tag{S2.3}$$

$$\begin{aligned}&\left(\hat{H}+\hat{H}_L+\hat{H}_T+\hat{H}_{an}\right)\cdot\left(\hat{y}\times\hat{m}\right)\\&=H\cos\theta\cos\phi\sin\theta_H+H_L\sqrt{\sin^2\theta+\cos^2\theta\cos^2\phi}+H_{an}\cos\theta\sin\theta\cos\phi.\\&=0\end{aligned}\tag{S2.4}$$

From experimental harmonic Hall voltage measurements, $V_{2f,//}$, $V_{2f,\perp}$, I_{ac}, θ_H, θ, R_{AHE}, and R_{PHE} are known. By solving the equations S1.4 and S2.1 ~ S2.4, H_L, H_T, ϕ, $\Delta\theta$, and $\Delta\phi$ can be obtained. The detailed procedures are listed in the following section S3.

S3. Measurements of R_{AHE} & R_{PHE} and procedures to evaluate H_L & H_T

The value of R_{PHE} is obtained by measuring the in-plane angular dependence of Hall voltage. With a magnetic field of 6 T applied in the film plane to fully saturate the magnetization along the field direction, the Hall voltage was recorded as a function of $\theta_{l\text{-}M}$ (the angle between the current and the magnetization) and its angular variation purely arises from the planar Hall effect. The representative R_H vs. $\theta_{l\text{-}M}$ is shown in Fig. S1(a). We measured R_{PHE} at different

temperatures for the temperature dependence of current induced effective fields as shown in Fig. S1(b).

By measuring out-of-plane anomalous Hall voltage loops, R_{AHE} is obtained at different temperatures. The temperature dependence of R_{AHE} is shown in Fig. S1(c). The ratio between R_{PHE} and R_{AHE} shows non-monotonic relationship with temperature.

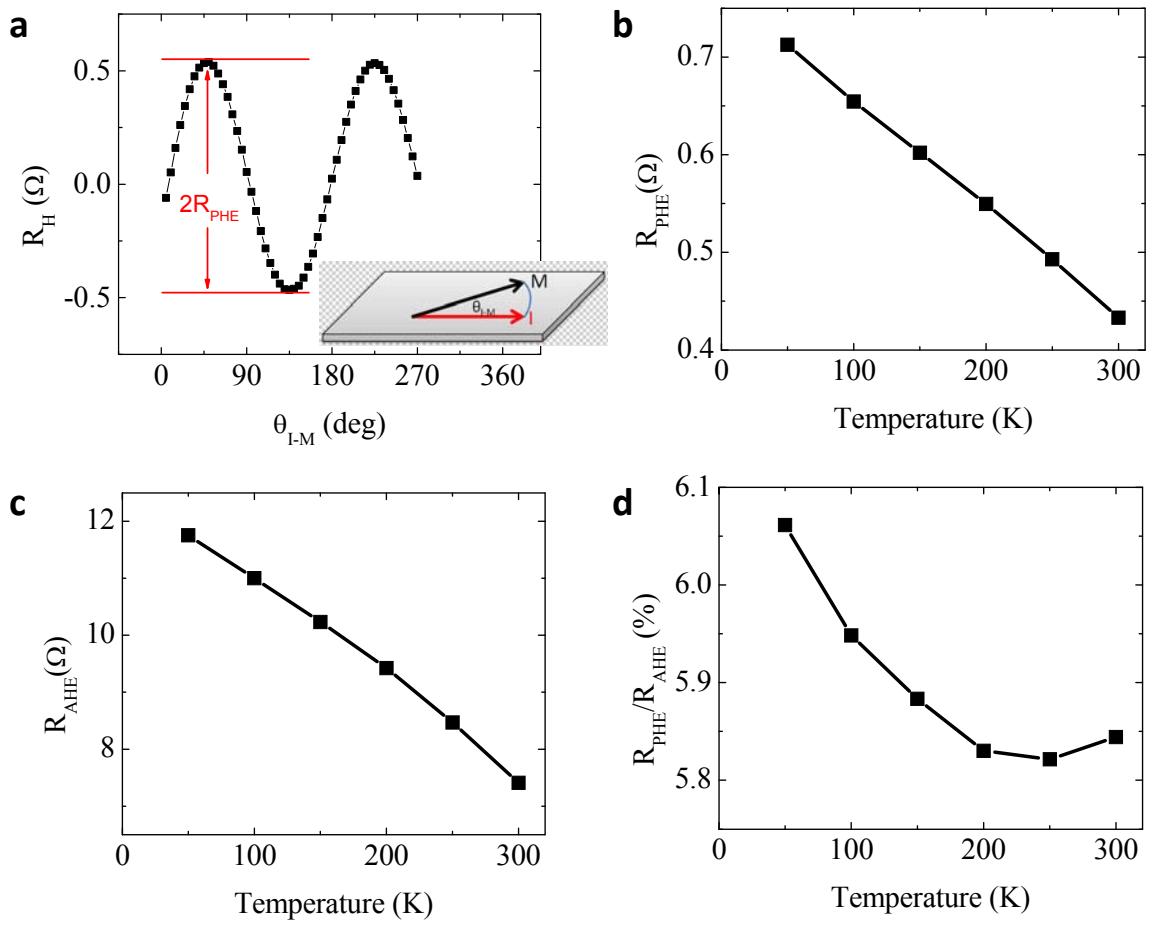

Fig. S1. (**a**) Example of R_H vs. $\theta_{I\text{-}M}$ for extracting R_{PHE}. Temperature dependence of R_{PHE} (**b**), R_{AHE} (**c**), and R_{AHE}/R_{AHE} (**d**).

With R_{PHE} and R_{AHE} obtained above and the equations developed in sections S1 ~ S2, we are able to evaluate H_L and H_T. Two approaches are performed. The first one is by assuming constant effective field values as shown in Fig. 2(e, f). The second one is calculating the

effective field values at each magnetic field. The detailed procedures of these two approaches are as follows.

(1) Fitting the $V_{2f,//}$ and $V_{2f,\perp}$ curves by assuming constant values of H_L and H_T

(a) Obtain θ at each applied magnetic field by using the first harmonic Hall voltage data. (The first harmonic Hall voltage loop does not depend on the measurement scheme, either longitudinal or transverse scheme, as concluded from the comparison at different temperatures)

(b) With an external magnetic field H applied at θ_H and the fitting parameters of H_L, H_T, and H_{an}, we can obtain $\theta_{//,+I}, \theta_{//,-I}, \theta_{\perp,+I}, \theta_{\perp,-I}, \phi_{//,+I}, \phi_{//,-I}, \phi_{\perp,+I}, \text{and}\, \phi_{\perp,-I}$ by solving equations (S2.1 ~ S2.4) (maximal positive and negative ac current need to be considered for each equation). The subscript of other parameters indicates the measurement scheme and the current direction, for example, $\theta_{//,+I}$ is the θ value in the longitudinal scheme with maximal positive ac current applied.

(c) Obtain R_{PHE} and R_{AHE} as describe earlier.

(d) Calculate $V_{2f,//}$ and $V_{2f,\perp}$ by using equation (S1.4):

$$V_{2f,//}(H) = -\frac{I_{ac}R_{AHE}\cos\theta(\theta_{//,+I} - \theta_{//,-I})}{4} - I_{ac}R_{PHE}\cos^2\theta\frac{(\phi_{//,+I} - \phi_{//,-I})}{2}$$

and

$$V_{2f,\perp}(H) = -\frac{I_{ac}R_{AHE}\cos\theta(\theta_{\perp,+I} - \theta_{\perp,-I})}{4} + I_{ac}R_{PHE}\cos^2\theta\frac{(\phi_{\perp,+I} - \phi_{\perp,-I})}{2}$$

Thus we can obtain the fitting curves of $V_{2f,//}$ and $V_{2f,\perp}$.

(e) The fitting parameters of H_L, H_T, and H_{an} are chosen for the best fitting to the amplitude and position of the peak in the experimental $V_{2f,//}$ and $V_{2f,\perp}$ curves.

(2) Calculation of angular dependent H_L and H_T

(a) Convert the field dependence of $V_{2f,//}$ and $V_{2f,\perp}$ curves into a θ dependence using the first harmonic experimental data.

(b) At each θ, one has the values of H, $V_{2f,//}$, $V_{2f,\perp}$, θ_H, H_{an}, H, I_{ac}, R_{AHE}, and R_{PHE}. H_{an} is obtained from the above assuming constant effective field values fitting.

(c) By solving equations of (S2.1 ~ S2.4) (maximal positive and negative ac current need to be considered for each equation) and (S1.4), one can obtain $\theta_{//,+I}, \theta_{//,-I}, \theta_{\perp,+I}, \theta_{\perp,-I}, \phi_{//,+I}, \phi_{//,-I}, \phi_{\perp,+I}, \phi_{\perp,-I}$ as well as H_L and H_T. Thus angular (θ) dependences of H_L and H_T are obtained.

S4. Linear correlation between current induced effective fields and I_{ac}

Harmonic loops are measured at 300 K to evaluate the current induced effective fields with different I_{ac}. H_L and H_T are obtained by using the method as in Fig. 2(e, f). As shown in Fig. S2, both H_L and H_T show a linear relationship with I_{ac}. The current (28.3 μA) used for the measurements in the main text is within the linear region where Joule heating is not playing a role.

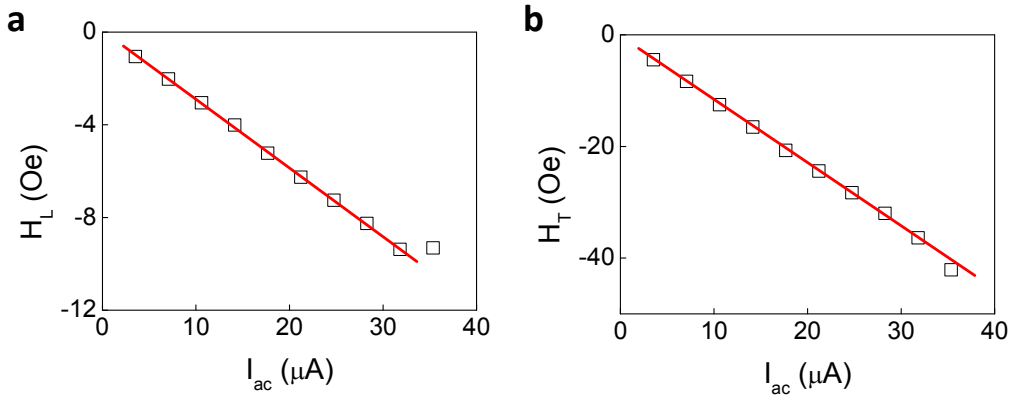

Fig. S2. Current induced effective fields vs. I_{ac}. H_L (**a**) and H_T (**b**) vs. I_{ac} at 300 K at $\theta_H = 1°$ from another device.

S5. Comparison of current induced effective fields in Ta/CoFeB/MgO and Pt/CoFeB/MgO

Current induced effective fields are compared between Ta/CoFeB/MgO and Pt/CoFeB/MgO nanowires (both of 600 nm width) by measuring current induced switching and harmonic anomalous Hall loops.

Figure S3(a, b) show the current induced switching in Ta and Pt nanowires at 300 K, respectively. With a 400 Oe external magnetic field applied along the current direction, R_H can be changed between a high and a low resistance state by an in-plane current, indicating the magnetization switching of the CoFeB layer between the $M_z > 0$ and $M_z < 0$. For the Pt nanowire, the switching occurs at ~ 1.3 mA, corresponding to a current density of 7.7×10^7 A/cm^2 assuming the current is flowing uniformly throughout the Pt/CoFeB layer. For the Ta nanowire, the switching current is ~ 0.11 mA which corresponds to a current density of 6.55×10^6 A/cm^2. In addition to the different switching current density for a Pt and Ta nanowire, the switching sequences are in the opposite sense for the Pt and Ta case indicated by the arrows in Fig. S3(a) and S3(b). The above observation suggests that the current induced effective fields responsible for the switching are opposite in Pt/CoFeB/MgO and Ta/CoFeB/MgO, as consistent with the opposite sign of the spin Hall angles in Pt and Ta.

To further confirm the opposite directions of effective field of H_L and H_T in Ta and Pt nanowires, we have performed the second harmonic anomalous Hall loop measurements in two geometries, as illustrated in Fig. 2(a) and 2(b) with $\theta_H = 1°$. The V_{2f} loops measured in the longitudinal geometry with currents collinear with fields for Pt and Ta nanowires are shown in Fig. S3(c) and S3(d), respectively. With field sweeps along the current flow direction, V_{2f} shows a positive (negative) peak at a positive (negative) magnetic field for a Pt nanowire, while it shows a negative (positive) peak at a positive (negative) magnetic field for a Ta nanowire, which

indicates the sign of H_L in the Pt case is opposite to that of a Ta nanowire. For the transverse component measurements, the magnetic field is applied perpendicular to the current flow, as shown in Fig. 2(b). In this case V_{2f} shows a positive peak at both polarities of magnetic fields from a Pt nanowire, while it shows negative peaks for a Ta nanowire, as shown in Fig. S3(e) and 2(f), indicating that the direction of H_T is opposite in the Pt and Ta case.

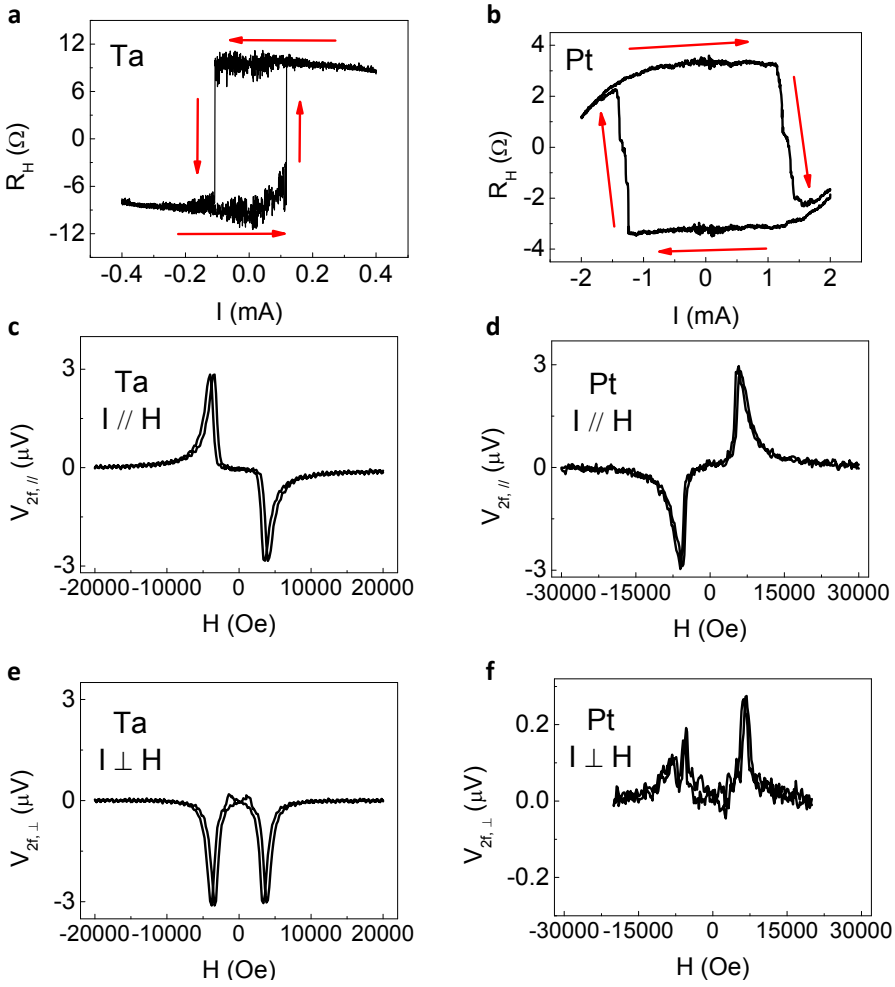

Fig. S3. Comparison of current induced switching and V_{2f} AHE loops in Ta and Pt nanowires. R_H vs. I for Ta (**a**) and Pt (**b**) nanowires. V_{2f} AHE loops with I_{ac} = 28.3 μA for Ta (**c, e**) and with I_{ac} = 70.7 μA for Pt (**d, f**) nanowires.

S6. Transport property Ta/CoFeB/MgO

The transport property of the device was studied by measuring the channel resistance ($R_{channel}$) and Hall resistance (R_H) with a 1 T magnetic field to saturate the magnetization out-of-film plane at different temperatures. Figure S4 shows $R_{channel}$ and R_H versus temperature. Both R_H and $R_{channel}$ show nonlinear behaviors with temperature. It should be noted that $R_{channel}$ mostly represents the property of the 2 nm Ta layer, since another metal layer CoFeB is only 0.8 nm thick.

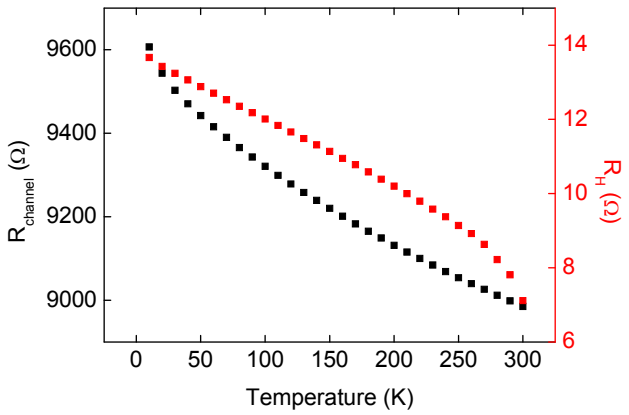

Fig. S4. Temperature dependence of $R_{channel}$ and R_H.

S7. Influence of PHE on evaluation of current induced effective fields

The influence of PHE on current induced effective fields at 300 K has been evaluated. In both approaches, either assuming the magnetization direction independent effective fields (Fig. S5(a)) or solving the effective fields at each magnetization direction (Fig. S5(b, c)), H_L and H_T are underestimated without consideration of PHE.

a

	With PHE correction	Without PHE correction
H_L	-7.4 Oe (-440 Oe per 10^8 A/cm^2)	-6.4 Oe (-381 Oe per 10^8 A/cm^2)
H_T	-32.7 Oe (-1942 Oe per 10^8 A/cm^2)	-32.1 Oe (-1907 Oe per 10^8 A/cm^2)

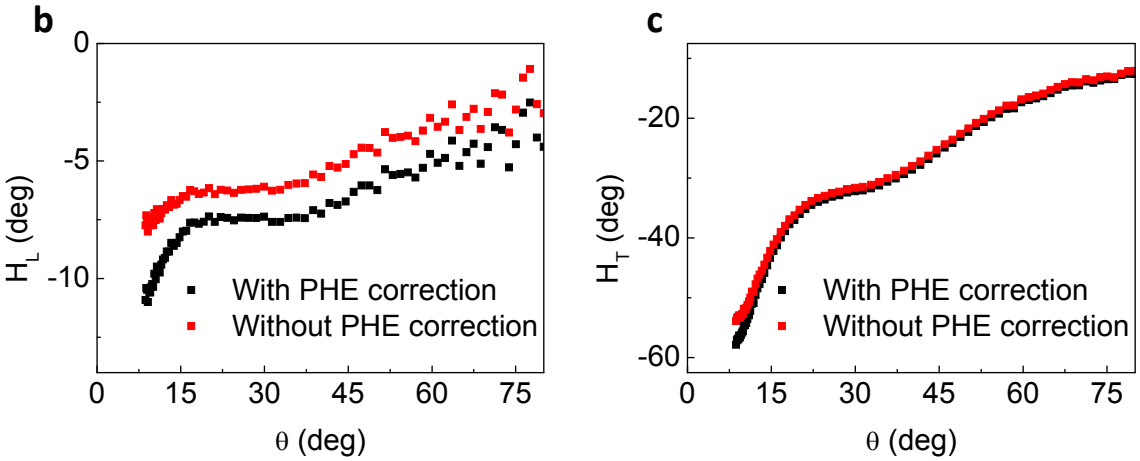

Fig. S5. Influence of PHE on evaluation of current induced effective fields at 300 K. (**a**) H_L and H_T by assuming independent effective fields on the magnetization direction, without and with consideration of PHE. (**b**) Angular dependence of H_L and H_T without and with consideration of PHE.

S8. Anomalous Nernst effect

Anomalous Nernst effect (ANE) also has contribution to the second harmonic voltage:

$$V_{2f}^{ANE} = V_{ANE}\frac{R_f}{2R_{AHE}} = V_{ANE}\frac{\sin\theta}{2}$$

We have measured the ANE contribution at different temperatures with field sweeping along the out-of-plane direction as shown in Fig. S6(a-d). The difference in V_{2f} at positive and negative saturated magnetic field is originated from the ANE, as current induced effective fields and Oersted field induced V_{2f} are symmetric to the out-of-plane field and thus their

contributions are excluded. By comparing V_{ANE}, $V_{2f,//}$, and $V_{2f,\perp}$, one can see that ANE contribution is very small.

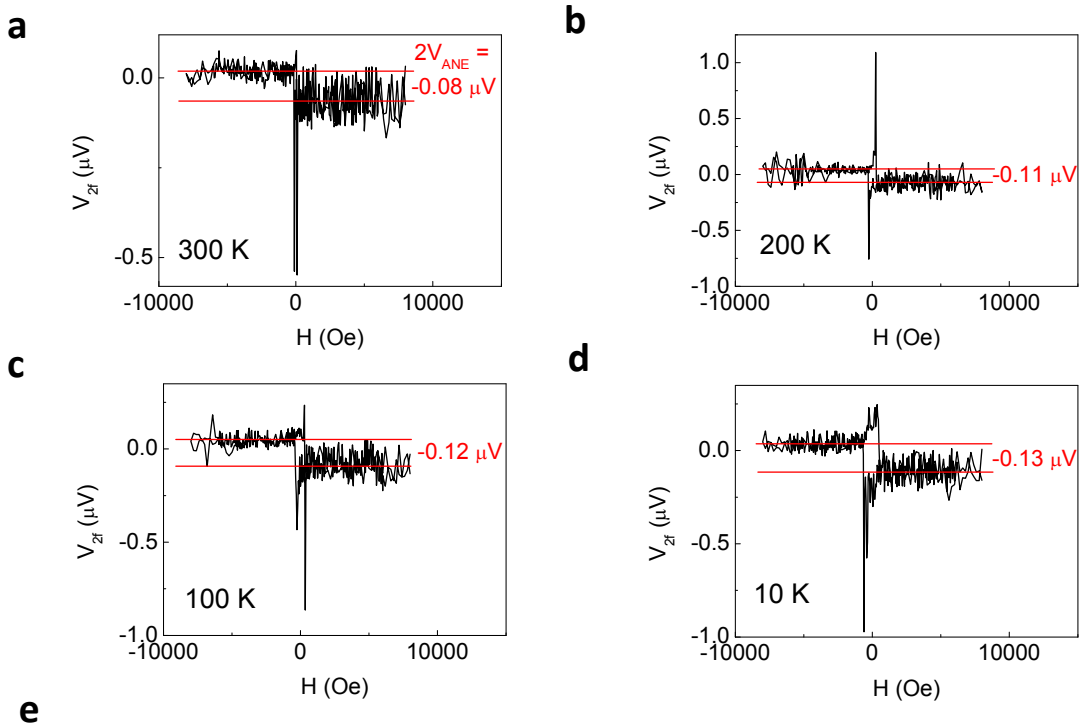

e

	$V_{\mathrm{ANE}}/2$ (μV)	Minimal $V_{2f,\parallel}$ (μV)	Minimal $V_{2f,\perp}$ (μV)
300 K	-0.02	-2.85	-3.1
200 K	-0.027	-1.54	-1.58
100 K	-0.03	-1.15	-0.67
10 K	-0.032	-0.95	-0.16

Fig. S6. ANE at different temperatures. (**a, b, c, d**) V_{2f} loops at out-of-plane direction at different temperatures. A 28.3 μA ac current is used for the measurements. (**e**) Comparison of V_{ANE}, $V_{2f,//}$, and $V_{2f,\perp}$ at different temperatures.